Nuclear fission: The "onset of dissipation" from a microscopic point of view

H. Hofmann,[1] F. A. Ivanyuk,[1,2] C. Rummel,[1] and S. Yamaji[3]
[1]*Physik-Department der TU München, D-85747 Garching, Germany*
[2]*Institute for Nuclear Research, 03028 Kiev-28, Ukraine*
[3]*Cyclotron Laboratory, Riken, Wako-Shi, Saitama 351-01, Japan*
(Received 9 February 2001; published 18 October 2001)

Semianalytical expressions are suggested for the temperature dependence of those combinations of transport coefficients that govern the fission process. This is based on experience with numerical calculations within the linear response approach and the locally harmonic approximation. A reduced version of the latter is seen to comply with Kramers's simplified picture of fission. It is argued that for variable inertia his formula has to be generalized, as already required by the need that for overdamped motion the inertia must not appear at all. This situation may already occur above $T\approx 2$ MeV, where the rate is determined by the Smoluchowski equation. Consequently, comparison with experimental results does not give information on the effective damping rate, as often claimed, but on a special combination of local stiffnesses and the friction coefficient calculated at the barrier.

DOI: 10.1103/PhysRevC.64.054316 PACS number(s): 24.10.Pa, 24.75.+i, 25.70.Jj, 25.70.Gh

I. INTRODUCTION

It is of considerable interest to understand the temperature dependence of transport properties associated with slow collective motion of large scale. Fission is a prime example, and indeed, for this case there is growing experimental evidence [1–5] that damping effectively increases with T. One often tries to characterize this feature by one parameter, the effective damping rate η that is related to the equation of average motion for a locally defined damped oscillator

$$M\frac{d^2q}{dt^2}+\gamma\frac{dq}{dt}+Cq(t)=0, \tag{1}$$

through

$$\eta=\frac{\gamma}{2\sqrt{M|C|}}. \tag{2}$$

The $q=Q-Q_0$ measures the deviation of the collective variable Q from some fixed value Q_0. In the following we will also need other combinations of inertia M, stiffness C, and friction γ, namely,

$$\tau_{\rm coll}=\frac{\gamma}{|C|}=\frac{\hbar}{\Gamma_{\rm coll}},\quad \tau_{\rm kin}=\frac{M}{\gamma}=\frac{\hbar}{\Gamma_{\rm kin}},\quad \text{and}\quad \varpi^2=\frac{|C|}{M}. \tag{3}$$

The $\tau_{\rm coll}$ sets the scale for (local) relaxation of collective motion in a given potential of (local) stiffness C. The $\tau_{\rm kin}$, on the other hand, measures the relaxation of the kinetic energy to the equilibrium value of the Maxwell distribution. Typically, for slow collective motion we expect this time to be smaller than the former. The limit of overdamped motion applies for $\tau_{\rm kin}\ll\tau_{\rm coll}$. Using the η introduced in Eq. (2), the following useful relation for their ratio is easily verified

$$2\,\eta=\frac{\Gamma_{\rm kin}}{\hbar\varpi}=\varpi\,\tau_{\rm coll}=\sqrt{\frac{\tau_{\rm coll}}{\tau_{\rm kin}}}. \tag{4}$$

For a positive stiffness ($C>0$) and underdamped motion, the ϖ would be the frequency of the vibration and the $\Gamma_{\rm kin}$ its width. It should be noted that in the literature a different notation is sometimes used where γ stands for η, and often the $\Gamma_{\rm kin}/\hbar$ is referred to as β.

To understand the dynamics in phase space one also needs the diffusion coefficients. At small temperatures they may deviate from the classic Einstein relation (see [6]), but these finer details will be neglected here. For such a situation the fission decay rate is commonly calculated within Kramers's "high viscosity" limit [7], for which the dependence on friction is given by

$$\frac{R_K^{hv}(\eta_b)}{R_K^{hv}(\eta_b=0)}=\sqrt{1+\eta_b^2}-\eta_b\equiv\left(\sqrt{1+\eta_b^2}+\eta_b\right)^{-1}. \tag{5}$$

Here, the index "b" refers to the fact that the transport coefficients are to be calculated at the barrier. It has been reported, see, e.g., Fig. 5 of [2], experimental data to suggest, when analyzed on the basis of Eq. (5), the η to be negligibly small at very low temperatures but to rise more or less sharply around $T\simeq 1$ MeV. This result is in qualitative agreement with microscopic calculations of the transport coefficients within linear response theory [6,8,9], although caution is still warranted here. Let us leave aside the fact that at lower temperatures the one-dimensional potential may attain more structure than that found in one minimum and one barrier, which is the picture underlying formula (5) and that for the sake of simplicity shall be applied in the sequel. As will be demonstrated below, even then it is not permissible to entirely parametrize the truly complicated transport process by the single quantity η. Rather, other combinations of M,γ, and C are needed for more realistic descriptions. Moreover, one should be guided by the theoretical fact, that not all transport coefficients are equally well accessible both theoretically as well as numerically, as is true for the inertia, for instance.

 ©2001 The American Physical Society

Unfortunately, when physicists address transport problems, all too often one disregards the importance of the inertia, and, in particular, its variation with the collective coordinate. Indeed, in studies based on the Caldeira-Leggett Hamiltonian (see, e.g., [10]) or in applications of the Random Matrix Theory (see [11]), the inertia is the one of the unperturbed collective part of the total Hamiltonian, treated as a (unknown) parameter. In the case of nuclear physics the situation is more complicated. First, there, no unperturbed inertia exists at all; it may only show up in the final effective equation of motion as one manifestation of the existence of collective dynamics. Second, the inertia M may depend sensitively on the collective degree of freedom. This feature is already well known from the traditional case of undamped motion at zero thermal excitation [12]. There is no *a priori* reason why this should be different at finite temperature, with perhaps two exceptions or modifications. With increasing T, the M gets close to the liquid drop value [13], which only varies smoothly with Q and which is quite small. Simultaneously the friction strength increases, so that one may quickly reach the situation of overdamped motion, for which no trace of the inertia can be seen anymore. Such features have been seen within the linear response approach (see [6]), but to the best of our knowledge no other transport model has so far addressed this question.

II. RATE FORMULAS

Like in the analysis underlying [3,4] we want to make use of a simple formula for the decay rate. In slight modification of Kramers's [7] classic one we write[1]

$$R_K^{hv}(\eta_b)=\frac{\varpi_a}{2\pi}\sqrt{\frac{M_a}{M_b}}\exp(-E_b/T)(\sqrt{1+\eta_b^2}-\eta_b). \quad (6)$$

The indices "a" and "b" refer to the minimum and maximum of the potential $V(Q)$, located at Q_a and Q_b, respectively. The E_b stands for the height of the barrier $E_b=V(Q_b)-V(Q_a)$. The factor $\sqrt{M_a/M_b}$, not contained in Kramers's original work, is meant to account for the modification one gets for variable inertia. Notice, that this inertia both influences the current over the barrier as well as the number of "particles" (phase space points) sitting in the well. Commonly both quantities are calculated with the same M that then drops out; see, e.g., Eqs. (4.30) and (4.31) of [10]. General reasons for the presence of this additional factor will be given in Appendix A. At first, in Sec. A 1 we follow the more common derivation involving the construction of the densities at the barrier and at the minimum, which in Sec. A 3 is reduced to the Smoluchowsky limit (see below). In Sec. A 4 we follow the arguments of Strutinsky [14], which lead to exactly the same formula. Unfortunately, in Ref. [14] this feature is disguised by the very fact that in the final expression Eq. (16), like in large parts of the derivation, primed and unprimed quantities are interchanged. It is for this reason that we feel compelled to redo the short calculation. The form (6) has recently been derived also in Ref. [15] by applying a generalized version of the "perturbed static path approximation (PSPA)."

[1]Since we are only looking at stationary situations we leave out the time dependent factor that sometimes is taken into account to simulate the "transient time" it takes before the stationary current has built up.

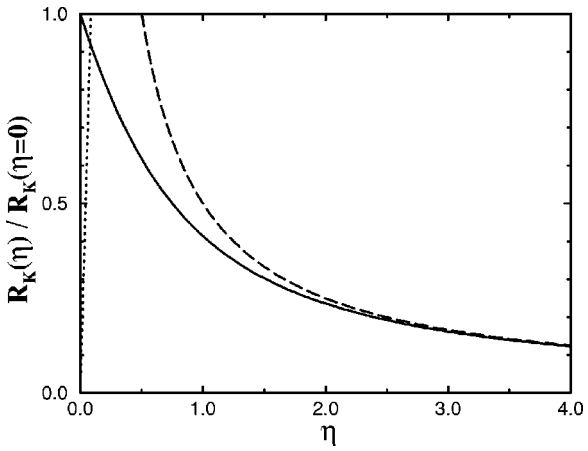

FIG. 1. Kramers's correction factor to the rate as a function of η: the solid and dotted curves correspond to the high [Eq. (5)] and low [Eq. (8)] viscosity limit (the latter is calculated for a barrier height of $E_b=5.8$ MeV, for ^{224}Th at 1 MeV) and the dashed ones to the overdamped limit (9).

Notice please that the dependence of the rate on the effective damping strength η_b still is given by Eq. (5). Using the relation $\varpi^2=|C|/M$ [see Eq. (3)] the limiting value at zero damping $R_K^{hv}(\eta_b=0)$ may be written in the two equivalent forms

$$R_K^{hv}(\eta_b=0)=\frac{\varpi_a}{2\pi}\sqrt{\frac{M_a}{M_b}}\exp(-E_b/T)$$

$$\equiv\frac{\varpi_b}{2\pi}\sqrt{\frac{C_a}{|C_b|}}\exp(-E_b/T). \quad (7)$$

The influence of dissipation is visualized by plotting in Fig. 1 the ratio $R_K^{hv}(\eta_b)/R_K^{hv}(\eta_b=0)$. In addition to the result of formula (5) we also show two other cases. First, we show a simplified version of the *low viscosity limit*

$$\frac{R_K^{lv}(\eta_b)}{R_K^{hv}(\eta_b=0)}=2\eta_b\frac{E_b}{T}. \quad (8)$$

It is valid for very small viscosity only [see Eq. (11) below] and provided [10] the action for the motion on top of the barrier may be approximated by $I(E_b)\approx E_b/\varpi_b$. As demonstrated in [8], for the nuclear case such a situation is found only at very small temperatures, much below the critical temperature for pair correlations to become important. Second, we explicitly indicate the limit that the ratio Eq. (5) takes on for overdamped motion

$$\frac{R_K^{hv}(\eta_b)}{R_K^{hv}(\eta_b=0)}=\frac{1}{2\eta_b} \quad \text{for} \quad \eta_b\gg 1. \quad (9)$$

Whenever the ''high viscosity limit'' applies, the influence of dissipation manifests itself in a reduction of the decay rate over the value given by Eq. (7). This deviation is claimed to allow for deducing a possible temperature dependence of dissipation through the ''measurable'' rate. It must be noted, however, that for overdamped motion it is not the effective damping factor η_b that one deduces. Indeed, overdamped motion is governed by the Smoluchowski equation in which no inertia appears (see Appendix A). But the latter not only is present in η_b but in $R_K^{hv}(\eta_b=0)$ as well. A better way of writing the rate formula in this case is

$$\begin{aligned} R_{\rm ovd} &= R_K^{hv}(\eta_b \gtrsim 1) \\ &= \frac{1}{2\pi}\sqrt{\frac{C_a}{|C_b|}}\frac{|C_b|}{\gamma_b}\exp(-E_b/T) \\ &\equiv \frac{1}{2\pi}\sqrt{\frac{C_a}{|C_b|}}\frac{1}{\tau_{\rm coll}^b}\exp(-E_b/T). \end{aligned} \tag{10}$$

Here, the time scale $\tau_{\rm coll}^b$ appears, which is relevant for overdamped motion across the barrier, see below. As can be inferred from Fig. 1 this limit is actually given for values of η_b just above unity. Notice, please, that it is only with the additional factor $\sqrt{M_a/M_b}$ included in Eq. (6), on top of Kramers's classic version, that the inertia drops out in the overdamped limit.

A few comments are in order on the validity of the rate formulas of the high viscosity limit, for which the following assumptions must hold true:

(1) On the way from the minimum to the barrier the temperature must not change.

(2) The barrier must be sufficiently pronounced, first of all in the sense that its height be large as compared to the temperature, viz., $E_b \gg T$, for further details see Sec. A 1.

(3) The effective damping rate must not be too small

$$\eta_b \geqslant \frac{T}{2E_b}, \tag{11}$$

otherwise formula (8) would have to be applied.

It may be quite a delicate matter to fix or calculate the temperature that is at stake here. For instance, a temperature T_{CN} associated with the *total* available energy for the *compound nucleus* might be much larger, as for high initial thermal excitations the system may cool down by emission of neutrons or γ's before it fissions. Finally, we should like to remark once more that presently any possible quantum features are discarded, which might show up at low temperatures [8].

III. MICROSCOPIC TRANSPORT COEFFICIENTS

Evidently, the temperature dependence of the rate will be greatly influenced by that of the transport coefficients—on top of the influence through the Arrhenius factor $\exp[-E_b(T)/T]$. Let us first look into results obtained applying linear response theory within the locally harmonic approximation [6], before we turn to discuss other forms used in the literature, such as in Ref. [4]. In this theoretical approach the transport coefficients of average motion are obtained by relating, in the low frequency regime the strength distribution of a microscopically calculated response function $\chi_{qq}(\omega)$ to the one of the damped oscillator. The latter is defined as

$$[\chi_{\rm osc}(\omega)]^{-1}q(\omega) \equiv -(M\omega^2 + i\gamma\omega - C)q(\omega) = -q_{\rm ext}(\omega), \tag{12}$$

and thus may be obtained by adding to Eq. (1) the term $-q_{\rm ext}(t)$ on the right and performing a Fourier transformation. For overdamped motion the response function turns into

$$\chi_{\rm ovd}(\omega) = \frac{i}{\gamma}\frac{1}{\omega + iC/\gamma}. \tag{13}$$

In accord with the remarks from above on the Smoluchowski limit no inertia appears anymore.

This approach permits one to calculate the transport coefficients as functions of shape and temperature for any given nucleus. The formulation is done in such a way that on top of shell effects and pairing (see [9] with references to previous works) collisional damping is accounted for as well (for a review see [6]). As one may imagine, such computations are quite involved, last but not the least because much knowledge is required about various aspects of the dynamics of complex nuclear systems. This is one of the reasons why, as yet numerical computations have been done only for particular nuclei or for more schematic cases [16,20,9]. Nevertheless, this experience may allow us to deduce some gross features that may be considered generic to a wider class of nuclear systems. This is what we are going to do below. It seems appropriate, however, to first add some general remarks concerning calculations based on the deformed shell model as an approximation to the general mean field.

The output of calculations of the type just mentioned contains much more detailed information than at present one may possibly relate to observable quantities. The coordinate dependence of the transport coefficients, for instance, is one prime example. Often in nuclear transport theories one simply has aimed at constant coefficients for inertia and friction. If calculated within the linear response approach, on the other hand, sizable variations with shape are seen. One may recall that a similar feature is already seen in the potential landscape, when calculated with the Strutinsky procedure, for instance. Besides the maxima and minima that are typical for gross shell effects, one sees detailed fine structure. Such features may depend on peculiarities of the underlying shell model, and may thus be unphysical in nature already by that reason. For the dynamic transport coefficients themselves, further implications arise from quasicrossings of levels. To large extent such effects can be expected to become much weaker in a multidimensional treatment, which, at present, is not feasible.

One should not forget that problems of this type are intimately related to the fact that transport coefficients of inertia, stiffness, and friction are those of *average motion, calculated on the level of the mean field*. Finally, however, they are needed for an equation of motion of Fokker-Planck type that

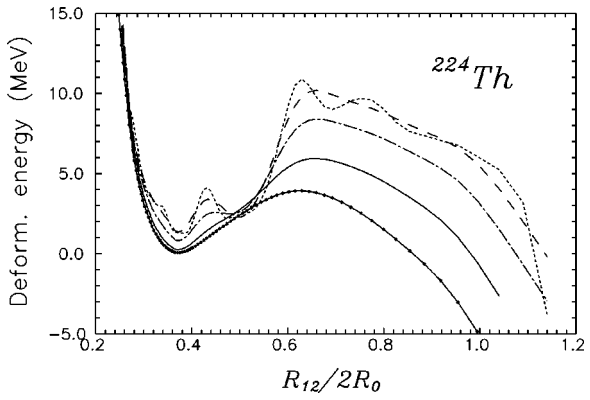

FIG. 2. Deformation dependence of the collective potential energy. The dotted curve shows the deformation energy at $T=0$. The dashed, dot-dashed, solid, and solid with stars curves correspond to the averaged deformation energy at temperatures $T=0$, 1, 2, and 3 MeV. The deformation parameter here is the distance R_{12} between the centers of mass of left and right parts of nucleus (divided by the diameter $2R_0$ of the sphere with equal volume). The averaging is carried out on the interval $\Delta(R_{12}/R_0)=0.1$.

accounts for dynamical *fluctuations*. The latter will help to smooth out the variations of the transport coefficients in most natural way. Evidently, the problem at stake here reflects the general deficiency of the mean field theory. In a more appropriate treatment one would be able to treat self-consistently both the mean field as well as its fluctuations. Since such a theory is not available we suggest some other, more pragmatic procedure. As described already, see, e.g., [9], one may smooth static energies as well as the other transport coefficients with respect to their dependence on deformation. The averaging interval in Q is to be chosen large enough to wash out the rapid fluctuations but small enough to preserve gross shell structures.

A. Shell effects on potential landscape

The static energy is calculated in the usual way as the sum of a liquid drop part and the shell correction, both of which depend on temperature, for details see [19]. An example of the deformation dependence of this potential energy is shown in Fig. 2. The dotted curve represents the case of zero thermal excitation. On top of the typical gross shell structure fluctuations of smaller scale are recognized as well. Features of this type lead to the rapid variations of the transport coefficients we talked about above; for the local stiffness as the second derivative of the static energy this is immediately evident. As mentioned, we consider such fluctuations as unphysical, for which reason we like to remove them by averaging over an appropriate interval ΔQ but to keep the gross shell structure. For the free energy, for instance, the smoothing can be done in the following way:

$$\langle \mathcal{F}(Q,T)\rangle_{\rm av}=\frac{\sum_i \mathcal{F}(Q_i,T) f_{\rm av}\left(\frac{Q-Q_i}{\Delta Q}\right)}{\sum_i f_{\rm av}\left(\frac{Q-Q_i}{\Delta Q}\right)}. \qquad (14)$$

The smoothing function $f_{av}(x)$ in Eq. (14) is taken to be that of the Strutinsky shell correction method and the Q_i are some points in deformation space. The use of the Strutinsky smoothing function guarantees stability of the averaging procedure: the smooth component of the deformation energy is restored after smoothing again. This implies that the liquid drop part of the energy is unchanged by this averaging.

In the figure we also show the averaged potential corresponding to temperatures $T=0$, 1, 2, and 3 MeV. As expected, with increasing temperature the deformation energy becomes much smoother and the height of the fission barrier gets reduced. This is due to the reduction of shell effects, as well as the temperature dependence of the liquid drop part. At temperatures above $T\approx 3$ MeV the shell effects have disappeared completely and the averaged deformation energy coincides with its liquid drop component. As seen from the figure, at smaller temperatures the shell correction, albeit averaged, does contribute to the deformation energy and, hence, to the stiffness. For example, at $T=1$ MeV the stiffness at the barrier (maximum of the deformation energy) is still several times larger than that of the liquid drop part.

It should be mentioned that in Ref. [18] a somewhat different (averaging) procedure was used. There the deformation energy was approximated by two parabolas and the stiffness (at the minimum and the barrier) was defined by the curvature of these parabola. In this way shell effects are washed out to a larger extent, not only with respect to the fine structure but even with respect to gross shell features. Consequently, the stiffness defined in this way is rather close to the liquid drop stiffness.

B. Temperature dependence of transport coefficients

1. Local stiffness

In the following we identify stiffness as the one corresponding to the free energy. Then we may write

$$C(T)=C_{\rm LDM}+\delta C(T). \qquad (15)$$

Here, $\delta C(T)$ represents the contribution from the shell correction, which disappears with increasing temperatures. To parametrize the latter feature we take over a formula of [21] to get

$$\delta C(T)=\delta C(T=0)\frac{\tau}{\sinh\tau} \qquad (16)$$

with the shell correction parameter

$$\tau=2\pi^2\frac{T}{\hbar\Omega_0} \quad \text{and} \quad \hbar\Omega_0=\frac{41\ \text{MeV}}{A^{1/3}} \qquad (17)$$

being the average shell spacing. Above $\tau_{\rm shell}\simeq 3-5$, which corresponds to a temperature of the order of

$$T_{\rm shell}\simeq(3-5)\frac{\hbar\Omega_0}{2\pi^2}\simeq 1-2\ \text{MeV}, \qquad (18)$$

the $\delta C(T)$ practically vanishes such that $C(T)$ attains its liquid drop value. Eventually, this $C_{\rm LDM}$ may still be treated as T dependent [22]. Finally, we should recall our suggestion from above to average the transport coefficients over smaller intervals in Q. In this sense the $\delta C(T=0)$ is meant to only represent gross shell features.

2. Local inertia

As mentioned already in the Introduction, one should expect the inertia to vary with temperature. It is more than tempting to assume a form similar to the one for the stiffness, namely,

$$M(T)=M_{\rm LDM}+\delta M(T) \tag{19}$$

in which the last term drops to zero as given in Eq. (16). Indeed, within the linear response approach a behavior of that type has been observed in a numerical study [13]. There, the value reached at larger temperatures was given by that of irrotational flow, which for the present notation means to identify $M_{\rm LDM}=M_{\rm irrot}$. To the best of our knowledge, there is no other theoretical model where such a transition is seen explicitly—although one must say that in phenomenological applications of transport models commonly the $M_{\rm irrot}$ is taken to represent the macroscopic value of inertia. At present the conjecture behind Eq. (19) still lacks a direct and general proof. However, in Ref. [23] the nucleonic response function has been studied applying periodic orbit theory (POT). There it was seen that its "fluctuating part" $\delta\chi(\omega)$ decreases with T like the shell correction to the static energy. For slow collective motion the inertia is determined by the second derivative of this response function with respect to frequency calculated at $\omega=0$ [see Appendix B and Eq. (B8) in particular]. Therefore, within such a model the "shell correction" to the inertia was indeed proven to behave as claimed above, although several questions remain open. Amongst others, it is unclear as to what extent this proof would get modified after considering "collisional damping." The latter cannot be treated within POT, but should play a major role for the transition to hydrodynamic behavior. Possible reasons for rendering a microscopic approach quite difficult have been reported in Refs. [18,19,6]. On the microscopic level they are related to the strength distribution for the local collective motion. The liquid drop model, on the other hand, represents motion of a system having a sharp surface, in contrast to microscopic calculations involving the diffuse surface of the mean field and, hence, of the density, for details see [19]. Fortunately, however, at larger T when the collisions become more and more important the motion gets strongly damped such that the inertia drops out anyway, see Eq. (13).

Owing to these difficulties in microscopic computations we propose to fix the $M(T)$ through the vibrational frequency ϖ and the local stiffness by the relation given in Eq. (3), namely, $M=|C|/\varpi^2$. For our version of Kramers's rate formula this was easily achieved in using the second variant shown in Eq. (7).

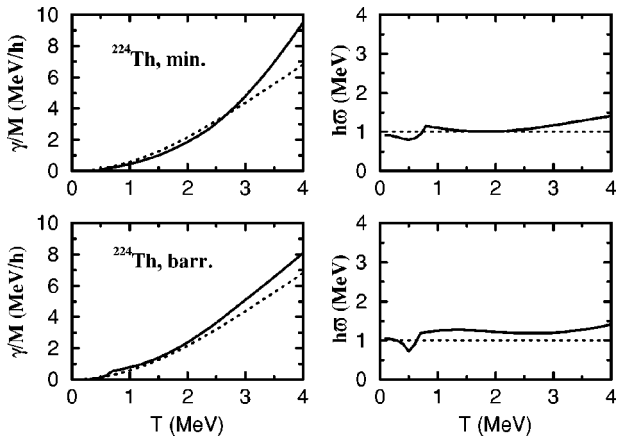

FIG. 3. Inverse relaxation time $1/\tau_{\rm kin}=\Gamma_{\rm kin}/\hbar$ (left panel) and $\hbar\varpi$ (right panel) as a function of temperature: the microscopic results (solid curves) compared to the approximations (20) and (21) (dotted curves).

3. Vibrational frequency

At the extremal points of the potential landscape this frequency ϖ is a well defined quantity. To some extent it is even accessible to experimental verification, at least for zero thermal excitation. At the minimum it may be associated with the energy of a collective mode (for very recent work on this subject see [24]) and for the barrier it influences the penetrability, as encountered, for instance, in neutron induced fission [25]. Generally, the $\hbar\varpi$ is believed to be of the order of 1 MeV. Indeed, numerical calculations for ^{224}Th [18,19] show this to be quite insensitive to temperature; to lesser extent this is true also for the variation with shape and mass number. Altogether, for a first orientation the following choice seems appropriate

$$\hbar\varpi_a\simeq\hbar\varpi_b\simeq 1\ \ {\rm MeV} \tag{20}$$

with deviations being within a factor of 2 or less. This appears to be the case even when pairing is included at smaller T. In Fig. 3 we take up the case of ^{224}Th, again. The calculation is the same as reported in Ref. [9]; more details will be given below in Sec. III B 6. From the right panel it is seen that this conjecture is pretty much fulfilled.

4. Ratio of friction to inertia

As said above, see Eq. (3), the ratio γ/M determines the inverse relaxation time to the Maxwell distribution. For underdamped motion this quantity also defines the width $\Gamma_{\rm kin}$ of the strength distribution. In Fig. 3 we show it on the left hand panel as function of T. The dashed curve represents the following approximation, details of which are discussed in Appendix B, namely,

$$\begin{aligned}\frac{\gamma}{M}\hbar&=\Gamma_{\rm kin}\\ &\approx 2\Gamma_{\rm sp}(\mu,T)\\ &=\frac{2}{\Gamma_0}\,\frac{\pi^2T^2}{1+\pi^2T^2/c^2}\approx\frac{0.6T^2}{1+T^2/40}\quad (T\ \text{in MeV}).\end{aligned} \tag{21}$$

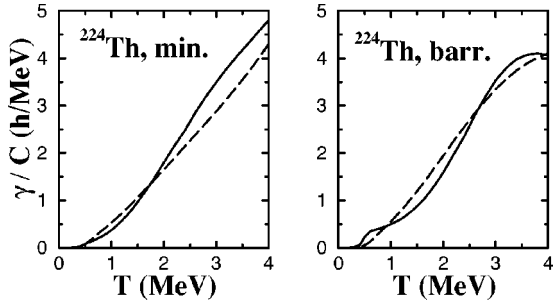

FIG. 4. Relaxation time $\tau_{\rm coll}$ for collective motion at the potential minimum and at the barrier: the microscopic result (solid curve) compared to the approximation [Eqs. (22)–(24)] (dotted curve).

As expected it represents the microscopic result quite well at smaller values of T that correspond to smaller values of damping. Recall, please, that the overdamped limit is given already for values of the damping factor η_b slightly above 1, see Fig. 1. As can be inferred from Fig. 3 and the estimate (20), this happens at temperatures above 2 MeV; mind that $\eta=(\gamma/M)(2\omega)^{-1}$.

5. Ratio of friction to stiffness

In Fig. 4 we plot, as function of T, the time $\tau_{\rm coll}=\gamma/|C|$, which measures the local relaxation in the coordinate. We may recall from Eq. (3) that for the overdamped case this is the only relevant time scale left. Its inverse determines the width of the strength distribution along the imaginary axis [see Eq. (13)]. Likewise the decay rate (10) associated to the Smoluchowski equation is proportional to $\tau_{\rm coll}^{-1}$. In Fig. 4, again, the fully drawn line shows the microscopic result. The dashed curves represent an approximation, into which the following two features are incorporated, the decrease of the stiffness [as given in Eqs. (15) and (16)] and the fact that with increasing T the friction coefficient reaches a plateau [17,18]. To combine both effects we chose a functional form similar to the one for the $\Gamma_{\rm kin}$ of Eq. (21) (see Appendix B) but with a different cut-off parameter $c_{\rm macro}$,

$$\tau_{\rm coll}=\frac{\gamma}{|C|}\approx\frac{2}{\hbar\varpi^2\Gamma_0}\,\frac{\pi^2T^2}{1+\pi^2T^2/c_{\rm macro}^2}$$

$$\approx\frac{0.6T^2}{1+\pi^2T^2/c_{\rm macro}^2}\,\frac{\hbar}{\rm MeV}\quad(T,c_{\rm macro}\ \text{in MeV}),\quad(22)$$

with $\hbar\varpi\approx1$ MeV. One should expect the $\tau_{\rm coll}$ to reach a macroscopic limit like

$$\tau_{\rm coll}\big|_{T_{hT}}=\left.\frac{\gamma(T)}{|C(T)|}\right|_{T_{hT}}\approx\frac{\gamma_{\rm wall}/2}{|C_{\rm LDM}(T)|},\qquad(23)$$

at larger temperatures. With a parametrization as in Eq. (22) the limit is obtained above $T_{hT}\simeq c_{\rm macro}/\pi$, for which reason the $c_{\rm macro}$ would be given by

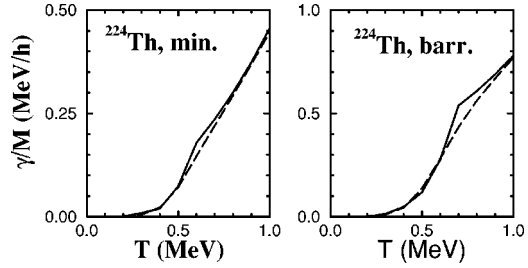

FIG. 5. Influence of pairing on the inverse relaxation time $\tau_{\rm kin}^{-1}=\Gamma_{\rm kin}/\hbar$. The microscopic results of [9] are compared with approximation (25).

$$c_{\rm macro}^2=\frac{\hbar\varpi^2\Gamma_0}{2}\,\frac{\gamma_{\rm wall}/2}{|C_{\rm LDM}(T)|}\approx8.2\,\frac{\gamma_{\rm wall}}{|C_{\rm LDM}(T)|}\,\frac{\rm MeV^3}{\hbar}.\qquad(24)$$

Here, we accounted for results obtained by several previous numerical calculations, see, e.g., [18,19,6]. They showed that the value of friction at large T is somewhat below the wall formula. The factor 1/2 is only to be considered a rough rule of thumb. For the stiffness, on the other hand, the macroscopic limit evidently is given by the liquid drop model. As the microscopic calculation was done with a T-dependent $|C_{\rm LDM}(T)|$ we chose the same one in this fit. In both curves the effects of pairing were included, which we are going to address now.

6. The influence of pairing

This problem has recently been studied in Ref. [9]. The fully drawn lines shown in the previous figures refer to such a calculation. Whereas in Ref. [9] one concentrated on the regime in which pairing is expected to be effective, the present results extend up to $T=4$ MeV. Calculations in that regime had been reported before in Ref. [19]. The underlying shell model is the same in both cases, but a different procedure is applied for the single particle width $\Gamma_{\rm sp}$. For the unpaired case the form (B11) was used, for which the frequency dependence of $\Gamma_{\rm sp}(\omega,T)$ leads to convolution integrals in the response functions. They are known to reduce the collective widths [6]. In the paired case such a calculation is no longer feasible, for which reason a constant $\Gamma_{\rm sp}(\mu,\Delta,T)$ had been assumed there, with Δ being the pairing gap. To have a more or less smooth transition to the unpaired case, we now approximate the $\Gamma_{\rm sp}(\omega,T)$ by the $\Gamma_{\rm sp}(\mu,\Delta,T)$ that above the critical temperature for pairing reduces to the $\Gamma_{\rm sp}(\mu,T)$ given in Eq. (B13). For this reason our present friction coefficient may be overestimated slightly. For $\Gamma_{\rm kin}/\hbar=\gamma/M$ the new results are shown in Fig. 5, where we concentrate on temperatures up to 1 MeV. To simulate the apparent effect of pairing to reduce friction we suggest the modified formulas

$$\frac{\gamma}{M}=f_{\rm pair}\frac{\gamma(\Delta=0)}{M(\Delta=0)}\equiv f_{\rm pair}\frac{\Gamma_{\rm kin}(\Delta=0)}{\hbar}\qquad(25)$$

and

$$\frac{\gamma}{|C|} = \tau_{\rm kin} = f_{\rm pair}\tau_{\rm kin}(\Delta = 0). \tag{26}$$

Here, $f_{\rm pair}$ parametrizes the decrease of friction due to pair correlations: An ansatz such as

$$f_{\rm pair} = \frac{1}{1 + \exp[-a(T - T_0)]} \tag{27}$$

may do with the following parameters: $a = 10$ MeV^{-1} and $T_0 = 0.55$ MeV at the barrier, and $a = 12$ MeV^{-1}, $T_0 = 0.48$ MeV at the minimum. It was found that this choice fits best the microscopic results [with the functional form (25)]. It is seen that these values vary with shape, which may be an indication that they are perhaps different for different nuclei. For a first orientation such details might be discarded. Then an average of the two values could be used both for a and T_0. Finally, we should like to remark that this influence of pairing is most dramatic for friction, and much less so for M and C. Therefore, we suggest to neglect the influence on the latter.

IV. TEMPERATURE-DEPENDENT DECAY RATES

If one wants to gain information on the transport coefficients and their T dependence, in particular, one needs to separate the influence of the prefactors from the more or less trivial exponential part (the ''Arrhenius factor''). Commonly, this feature is then simply identified by Kramers's conventional factor that only depends on η_b. A systematic study performed in Ref. [26] has revealed the appearance of a *threshold temperature* $T_{\rm thresh}$ above which deviations from the statistical model are seen over a wide range of fissioning systems. Moreover, its ratio over the temperature-dependent barrier heights $E_{\rm Bar}(T) \equiv E_b(T)$ showed a remarkable insensitivity on mass number A. For later purpose it is more convenient to divide that ratio by 2 to get

$$\left.\frac{T}{2E_b(T)}\right|_{\rm thresh} \simeq 0.13 \tag{28}$$

from Fig. 4 of [26]. We are now going to view this result in the light of our microscopic transport coefficients. At first we shall concentrate on the ratio $R_K^{hv}(\eta_b)/R_K^{hv}(\eta_b = 0)$, to comment later on the T dependence of the additional factors seen in Eq. (7), and which involve ratios of the inertias or stiffnesses.

A. Rate from microscopic transport coefficients

In Fig.6 we plot the normalized rates for the three cases shown already in Fig.1, but now as function of temperature as determined by our microscopic $\eta(T)$. Various conclusions may be drawn from this figure.

(1) Above $T \simeq 0.6 - 0.7$ MeV an ''onset of dissipation'' is seen, indeed, in the sense of a decrease of the rate for the ''high viscosity'' limit. The value of this ''threshold temperature'' is in reasonable agreement with the $T_{\rm thresh} \simeq 1.09 - 1.22$ given in Table I of [26] for ^{224}Th.

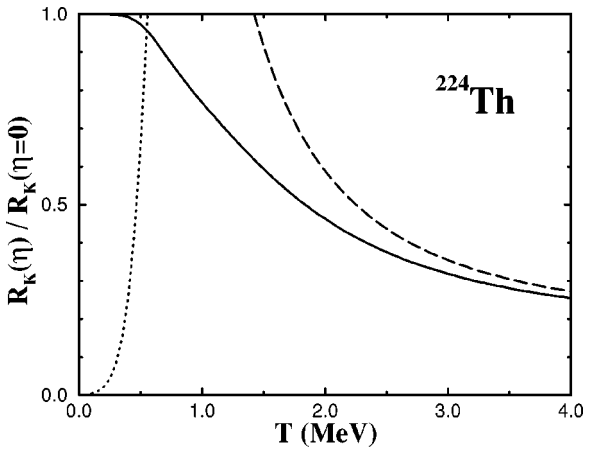

FIG. 6. Temperature dependence through a microscopic $\eta = \eta(T)$ (solid line); the dashed curve represents the overdamped case as given by Eq. (9), the dotted one corresponds to the low viscosity limit as given by Eq. (8) for the same barrier height as in Fig. 1.

(2) Moreover, from the right panel of Fig. 5 together with the value for the frequency given in Fig. 3 one may deduce for these temperatures the η_b to be larger than the value of $T/2E_b$ given in Eq. (28). It then follows from Eq. (11) that the deviation from the statistical model is to be attributed to the high viscosity limit.

(3) This feature evidently is related to the disappearance of pair correlations at $T \simeq 0.5$ MeV. The curve for the ''low viscosity limit'' demonstrates that below this temperature the former case should not be used at all [mind condition (11)].

(4) As indicated earlier, above $T \simeq 2$ MeV the overdamped limit applies, for which we suggested to use formula (10).

B. Comparison with phenomenological models

In Fig. 7 we compare the result shown in the previous figure [for formula (5)] with the one of a macroscopic pic-

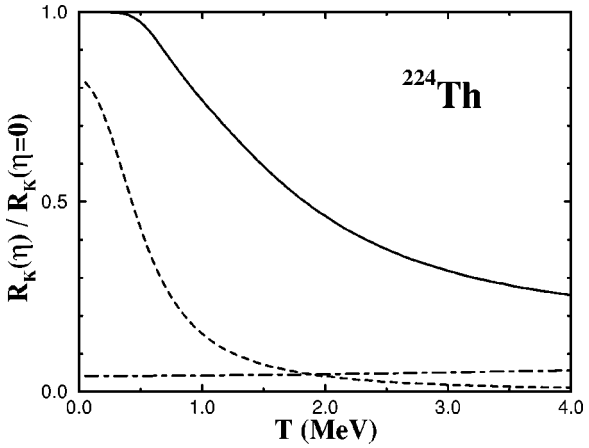

FIG. 7. Temperature dependence of the decay rate in high viscosity limit: solid curve: same as in Fig. 6; dashed curve: η_b given by Eq. (29); dashed-dotted curve: wall friction and liquid drop values for stiffness and inertia.

ture, together with that suggested in Refs. [3,4]. By the macroscopic model we mean to use the wall formula for friction, the liquid drop model for inertia (irrotational flow) as well as for the stiffness. In Ref. [3] the following functional form for $\eta_b(T)$ had been suggested:

$$\eta(T)=0.2+3T^2. \tag{29}$$

It is seen that for such a T dependence the onset of dissipation occurs quite abruptly and at rather small temperatures. One must have in mind, though, that the ratio plotted in Fig. 7 is sensitive to the temperature at the barrier, as it is this one that determines the η_b. This fact might explain why the transition exhibited here through the dashed curve lies at smaller T than discussed in Refs. [3,4]. It can be said that for the other ansatz $\eta(T)=0.2+5T$ used as well the transition would occur at even smaller temperatures. The reason seems obvious: In these two forms *the dissipation rate* η *is much too large at small* T—at least too large as compared to our microscopic results. Indeed, as discussed above, at small temperatures *pairing correlations require dissipation to vanish*.

C. Relation to the statistical model

The rate of the high viscosity limit when extrapolated down to zero friction, $R_K^{hv}(\eta_b=0)$, corresponds to a variant of the transition state method, and thus to one [7] of the Bohr-Wheeler formula [27] (see also [14]). We demonstrate in Sec. A 2 that this still holds true for the modified version of variable inertia. One must have in mind, however, that such an extrapolation may be meaningless as, by its very construction, the transition state method bases on the assumption of a complete equilibrium. The latter is given only if sizable friction forces provide sufficiently fast relaxation to this global equilibrium. Our result for the temperature dependence of friction then imply that any version of the transition state result must be taken with reservation when applied at small thermal excitations. At this point it would be too much to compare complicated evaluations of the Bohr-Wheeler formula with estimates of Kramers's rate which have our microscopic transport coefficients as input. This must be subject of further studies.

What is feasible, however, is to compare our results with those of a statistical model, in which the Bohr-Wheeler formula [27] is approximated by

$$R_{stat}=\frac{T}{2\pi\hbar}\exp(-E_b/T), \tag{30}$$

see, e.g., [28,29]. This approximate form comes up when in the Bohr-Wheeler formula [27] the level density at the barrier is identified as that of the total system, whereas in the correct expression the collective degree of freedom has to be excluded (see, e.g., [14]). That such an approximation may lead to erroneous results when interpreting data has been pointed out also in Ref. [30]. We may briefly follow up this discussion by using our microscopic input.

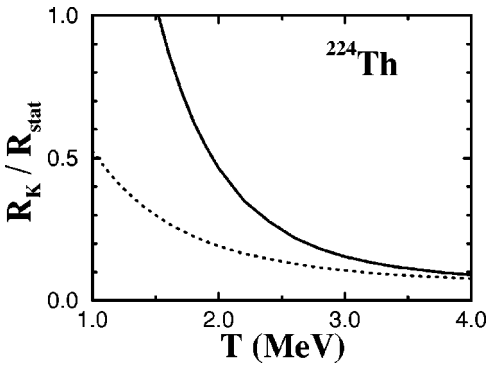

FIG. 8. Ratio (32) of Kramers's rate to that of the statistical model (solid line). The dotted curve demonstrates the influence of the stiffnesses, which now are calculated from the liquid drop model, but with friction unchanged.

The ratio R_K/R_{stat} may be calculated for the three cases we looked at before, low and ''high viscosity'' limit as well as the overdamped limit. For ''high viscosity'' one gets from Eq. (6) [mind Eq. (7)]

$$\frac{R_K^{hv}}{R_{stat}}=\frac{\hbar\varpi_b}{T}\sqrt{\frac{C_a}{|C_b|}}(\sqrt{1+\eta_b^2}-\eta_b). \tag{31}$$

For overdamped motion, expression (10) leads to

$$\frac{R_K}{R_{stat}}=\sqrt{\frac{C_a}{|C_b|}}\frac{|C_b|}{\gamma_b}\frac{\hbar}{T}. \tag{32}$$

The result (30) can be expected to deviate sizably from Kramers's one. This is demonstrated in Fig. 8 by the fully drawn line that represents the ratio given in Eq. (31). Here, the ''onset of dissipation'' seemingly is even more pronounced, and the deviation starts at a much higher temperature. However, *these effects are not related to dissipation only*. Besides the more or less obvious fact of the prefactor in Eq. (30) being not identical to the frequency $\hbar\varpi_a\simeq\hbar\varpi_b$, there appears the square root of the ratios of the two stiffnesses. The latter is largely influenced by shell effects, which are known to be sensitive to variations of temperature. The implication of this feature on the ratio R_K/R_{stat} is exhibited in Fig. 8 by the dotted curve. Its deviation from the solid one is solely due to the stiffnesses being evaluated from the (T-independent) liquid drop model $C_{\rm LDM}(T=0)$.

Obviously, the R_{stat} becomes small at small temperatures, say below about 0.5 MeV. In this range nuclear friction is small, too, not only at the barrier but also inside the well (see Figs. 3 and 4). Discarding any quantum effects, which in this regime may become important [8], one might then use Kramers's low viscosity limit. As mentioned previously, any transition state result, however, does *not apply, for which reason a comparison of both is meaningless*. For the Bohr-Wheeler formula to be valid the system inside the well has to be in *complete equilibrium* [10]. Such a situation is given only for sufficiently large damping.

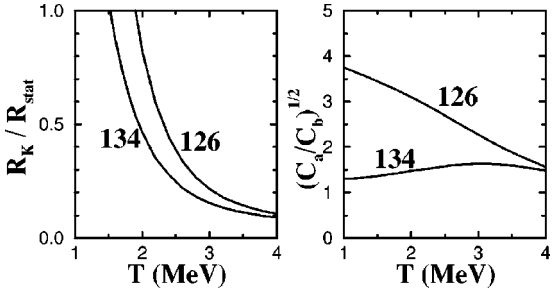

FIG. 9. Results for different Th isotopes: left panel: ratio of Kramers's rate to that of the statistical model; right panel: influence of shell structure through ratio of stiffnesses.

D. Isotopic effects

In Ref. [3] different nuclei have been studied experimentally and analyzed with respect to a temperature dependence of the dissipation strength η_b (called γ there). In particular two isotopes of thorium have been examined, namely, ^{224}Th and ^{216}Th corresponding to neutron numbers of $N=134$ and 126, respectively. The different behavior seen in experiment has been fully attributed to this η_b and in this way very different values of η_b have been found, together with a different increase with T. Evidently such features cannot be explained within a macroscopic picture. One needs to account properly for shell effects. From our experience with microscopic computations it seems unlikely that they would have such a big influence on friction alone. On the other hand, recalling that $N=126$ corresponds to a closed shell, it is evident that the stiffnesses for $N=134$ and 126 will be quite different, in particular for the ground state minimum. This effect can be seen on the right panel of Fig. 9, which shows the square root of the relevant ratios to be quite different for the two isotopes. Moreover, it is easy to convince oneself that this effect is in the right direction. Indeed, as can be seen from Eq. (31), smaller values of this ratio $\sqrt{C_a/|C_b|}$ *simulate* larger values of η_b. Notice, please, that an excitation of about 100 MeV, as given in Fig. 9 of Ref. [3], corresponds to a temperature of $T\approx 2$ MeV. Finally, on the left panel in Fig. 9 we show the full ratio as given by Eq. (32). Evidently, we are not able to fully explain the results shown in Fig. 9 of Ref. [3], but this would have been asking too much, for various more or less obvious reasons.

V. SUMMARY AND DISCUSSION

One of our main goals was to suggest simple forms of the temperature dependence of those quantities that parametrize transport in collective phase space. These suggestions are based on simplified pictures for the intrinsic response combined with experience in microscopic computations within realistic approaches employing the deformed shell model. Rather than using the transport coefficients themselves we argued in favor of combinations that allow for a more direct physical interpretation.

These results were tested at the fission decay rate. To make our reasoning as transparent as possible, a simple one-dimensional model was used, for which Kramers's picture can be applied. This model is somewhat schematic, in so far as the potential is assumed to have one pronounced minimum and one pronounced barrier only, which follow more or less closely the form of two oscillators, one upright and one inverted. Different to the original work of Kramers's and of many subsequent applications, our transport coefficients were allowed to vary along the fission path. In a first approximation this leads to a modification of Kramers' original rate formula. For variable inertia, such a modification already appears necessary for the simple reason that for large damping one should reach the rate formula corresponding to the Smoluchowski equation. Still, the deviation from the undamped case is solely determined by the damping strength η_b calculated at the barrier. However, for a complete understanding of temperature effects of the decay rate it does not suffice to concentrate only on this damping strength.

Of course, such a simple model for the static energy may not apply at all at (smaller) temperatures when shell effects lead to important deviations. It is unclear how one could generalize the formulas of Kramers and Bohr-Wheeler to realistic cases with two or perhaps three barriers having minima in between. To calculate the decay rate for such potentials it is perhaps simpler to use the more general description in terms of Fokker-Planck or Langevin equations. It may then also be possible to account better for the variations of the other transport coefficients with coordinate and temperature, namely, inertia and friction. To the best of our knowledge, in such calculations only the transport coefficients of macroscopic models have been used so far. However, the content of Fig. 7 indicates that greater deviations can be expected for microscopic inputs.

Nevertheless, within our model we are able to clarify a few important points that must not be discarded even at temperatures at which shell effects do not really dominate the process.

(1) The transition to overdamped motion already occurs at temperatures around $T\simeq 2$ MeV. Then the decay rate should be calculated from the Smoluchowski equation.

(2) In this case no inertia appears any more. Thus neither the frequency ϖ nor the effective width $\Gamma_{\rm kin}=\hbar\gamma/M$ (sometimes referred to as $\hbar\beta$) play any role.

(3) The solely important quantities are the ratio of friction to stiffness, γ/C, and (for the decay rate) the ratio C_a/C_b of the stiffnesses. Physically, the former determines the relaxation time for sliding motion in the potential, see Eq. (22). In passing, we may note that it is essentially this time that determines the saddle to scission time, an effect not considered here. Notice that these stiffnesses are subject to large shell effects that may easily be accounted for by the shell correction method. As a first demonstration of this effect we have calculated the impact of these stiffnesses on the decay rate of the thorium isotopes $N=134$ and $N=126$.

(4) In principle, the vibrational frequency ϖ should be obtained from microscopic computations (for $T<2$ MeV). But a simple and quite fair estimate may be given by $\hbar\varpi_a \simeq \hbar\varpi_b \simeq 1$ MeV, Eq. (20), which is almost exact for the case of ^{224}Th. Evidently, the ϖ may be greatly influenced by shell effects, but from our experience we claim that the deviations are within a factor of about 2.

(5) Finally, we should like to briefly comment on the pa-

per presented in Ref. [31]. There scaling rules have been derived for the case of the Smoluchowski equation, and based on phenomenological input. In the schematic model underlying the discussion a few assumptions had been made which are not in accord with microscopic results. First of all, the ratio of barrier height to temperature definitely decreases with T. Secondly, as the authors monitor themselves, a frequency at the barrier of the order of 20 MeV is much too high. Together with the value used for β, namely, $\beta \equiv \Gamma_{\rm kin}/\hbar \simeq 10^{22}$ sec^{-1} one gets an $\eta_b \simeq 0.2$. This implies the motion around the barrier to be *under* damped rather than overdamped. Moreover, for several cases studied in this paper, the η_b is seen to be of the order of or even smaller than $T/2E_b$. Thus, according to Eq. (11) not even Kramers's high viscosity limit seems appropriate.

Let us turn now to very low temperatures, say to the regime where pairing correlations become important. They imply an additional reduction of dissipation, such that one may truly speak of the onset of dissipation when pair correlations disappear. It must be said though that this transition occurs at temperatures definitely smaller than those suggested in [1–5]. As mentioned earlier, one has to make sure, however, that one speaks of the same temperature. The one of the compound nucleus might be larger than the one the system still has when it passes the barrier.

It needs to be stressed that a small damping strength at small temperatures may have quite drastic implications. In case the ''high viscosity limit'' still applies quantum corrections to the decay rate would lead to an increase of the latter [8]. If, however, the dissipation strength falls below the limit given by Eq. (11) the nature of the diffusion process would change completely. Then dissipation is too weak to warrant relaxation to a quasiequilibrium. This not only violates Kramers's rate formula (for the high viscosity limit), or our extension of it, but also the Bohr-Wheeler formula becomes inapplicable. Moreover, so far no method exists as to how one might incorporate collective quantum effects.

Finally we should like to indicate that our transport coefficients are not free of uncertainties in some of the parameters specifying our microscopic input. The most difficult one is found in the single particle width. It has been parametrized in Ref. [32] by referring to the optical model for nucleons in finite nuclei through a kind of local density approximation. There the Γ_0 and its dependence on the nuclear density had been traced back to microscopic computations of the self-energies in a generalized Brueckner-type description. This implies an uncertainty of perhaps a factor of 2 in all formulas where the friction coefficient appears, as in Eq. (21) or Eq. (22) as well as in the η of Eq. (4). Since any microscopic answer on such questions is extremely difficult, there is hope of narrowing down this uncertainty by more elaborate comparisons with experimental results.

ACKNOWLEDGMENTS

The authors gratefully acknowledge financial support by the Deutsche Forschungsgemeinschaft and are grateful to J. Ankerhold, B. Back, A. Kelic, and M. Thoennessen for enlightening discussions. Two of us (F.A.I. and S.Y.) would like to thank the Physik Department of the TUM for the hospitality extended to them during their stay.

APPENDIX A: IMPLICATIONS FROM A VARIABLE INERTIA

In Kramers's seminal paper [7] the equation for the density in phase space was written and applied to the decay of a metastable system for the case of constant transport coefficients. In nuclear physics both the inertia as well as the friction coefficient vary with the collective coordinate. This has been accounted for already in early applications to heavy ion collisions, where globally Gaussian solutions (centered at the classical trajectories) were used to calculate reaction cross sections see, e.g., [33]. Written in compact form for one variable the transport equation should read

$$\frac{\partial}{\partial t} f(Q,P,t) = \left\{ -\frac{P}{M(Q)}\frac{\partial}{\partial Q} + \frac{\partial}{\partial Q}\left(\frac{P^2}{2M(Q)} + V(Q)\right)\frac{\partial}{\partial P} + \frac{\partial}{\partial P}\left(\frac{P}{M(Q)}\gamma(Q) + D(Q)\frac{\partial}{\partial P}\right)\right\} f(Q,P,t). \tag{A1}$$

Neglecting any quantum effects, which might show up at small temperatures only [6,8], the diffusion coefficient is given by the classic Einstein relation $D(Q) = \gamma(Q)T$. A possible T dependence of the transport coefficients has not been indicated explicitly. This is immaterial as long as we treat temperature as a fixed parameter, which is assumed to hold true in the entire paper. As is easily verified, one stationary solution of Eq. (A1) is the distribution of global equilibrium

$$f_{\rm eq}(Q,P) = \frac{1}{Z}\exp[-\beta \mathcal{H}(Q,P)] \tag{A2}$$

with the energy given by the classical Hamilton function

$$\mathcal{H}(Q,P) = \frac{P^2}{2M(Q)} + V(Q). \tag{A3}$$

The reason is due to the following features: (i) The conservative part of the equation has the form of Liouville's equation, namely,

$$\frac{\partial}{\partial t} f(Q,P,t) = \{\mathcal{H}(Q,P), f(Q,P,t)\}. \tag{A4}$$

(ii) The terms that represent dissipative and fluctuating forces are assumed independent of the momentum P, such that P only appears quadratically in the kinetic energy. (iii) The choice of the diffusion coefficient by $D(Q) = \gamma(Q)T$ makes the second line of Eq. (A1) vanish once applied to Eq. (A2).

The structure of these equations not only allows for the proper equilibrium, but it also warrants the continuity equation to be valid in the form

$$\frac{\partial}{\partial t} n(Q,t) + \frac{\partial}{\partial Q} j(Q,t) = 0, \tag{A5}$$

with the current and spatial densities being defined as

$$j(Q,t)=\int dP\,\frac{P}{M(Q)}f(Q,P,t) \tag{A6}$$

and

$$n(Q,t)=\int dP f(Q,P,t), \tag{A7}$$

respectively. This is easily verified with the help of Eq. (A1) exploiting partial integrations with respect to momentum P (for which no ''surface terms'' survive).

Both in Liouville's equation as well as in the transport equation (A1) a term appears that needs to be treated with special care. It is the one that results from the spatial derivative of the kinetic energy, and reads

$$\left(\frac{\partial}{\partial Q}\,\frac{P^2}{2M(Q)}\right)\frac{\partial}{\partial P}f(Q,P,t). \tag{A8}$$

Indeed, this term is absent in the common derivation of the rate formula (see, e.g., [10]), where always a constant inertia is assumed to be given. It may be noted that this term may imply difficulties with ''saddle point approximation,'' as needed in Kramers's stationary solution. Moreover, and more important for the present purpose, this term is also neglected in extracting the transport coefficients within the linear response approach. There, a locally harmonic approximation is exploited, which for the sake of simplicity is formulated only with respect to the coordinate. What that means may be visualized in the following way. Look at the Liouville part of the transport equation, in particular, at the term that involves the derivative of the Hamilton function with respect to Q. First of all there is the ordinary force from the potential, which in the expansion around a Q_0 to harmonic order may be written as

$$-\frac{\partial}{\partial Q}V(Q)\equiv K(Q)\approx K(Q_0)-C(Q_0)(Q-Q_0), \tag{A9}$$

with the second derivative of the potential defining the local stiffness $C(Q_0)$. In addition there is the term

$$\left(\frac{\partial}{\partial Q}\,\frac{P^2}{2M(Q)}\right)=P^2\frac{\partial}{\partial Q}\left(\frac{1}{2M(Q)}\right) \tag{A10}$$

which is of second order (namely, in P). In a consistent treatment one would have to introduce a P_0 and expand all terms locally in collective phase space around the (Q_0,P_0) to second order both in $Q-Q_0$ and $P-P_0$ (see [33]). So far this has not been done when extrapolating transport coefficients from the microscopic linear response approach. This does not imply that our inertia may not change with the coordinate at all. It only means that the terms including its derivative have been discarded. With respect to the basic transport equation (A1) this approximation may be phrased as

$$\left|\left(\frac{\partial}{\partial Q}\,\frac{P^2}{2M(Q)}\right)\frac{\partial}{\partial P}f(Q,P,t)\right| \ll\left|\frac{\partial}{\partial P}\left(-K(Q)+\frac{P}{M(Q)}\,\gamma(Q)\right)f(Q,P,t)\right|. \tag{A11}$$

1. Kramers's decay rate formula extended to variable inertia

For reasons given above, we still want to make use of the condition (A11). Nevertheless, it is necessary to rederive an expression for the rate, which still is defined as

$$R=\frac{j_b}{N_a}. \tag{A12}$$

To calculate the quantities involved we need a global solution $f_{\rm glob}(Q,P)$ of equation (A1), which corresponds to a small but finite, (quasi)stationary current across the barrier. This current may be calculated from Eq. (A6), with $f(Q,P,t)$ replaced by $f_{\rm glob}(Q_b,P)$. The probability N_a of finding the system inside the well at Q_a may be calculated as follows:

$$N_a=\int_{Q_a-\Delta}^{Q_a+\Delta}dQ\int dP f_{\rm glob}(Q,P)=\int_{Q_a-\Delta}^{Q_a+\Delta}dQ n_{\rm glob}(Q). \tag{A13}$$

The integration range 2Δ has to be smaller than Q_b-Q_a but large enough such that it contains the vast majority of the ensemble points sitting in the well. An approximation for $f_{\rm glob}(Q,P)$ may be constructed by matching together at some intermediate point $\overline{Q}$ local solutions valid at the minimum Q_a and at the barrier Q_b. The global solution $f_{\rm glob}(Q,P)$ will have an overall normalization factor that drops out when calculating the rate from Eq. (A12). The normalization of the local solutions $f(Q\approx Q_a,P)$ and $f(Q\approx Q_b,P)$, on the other hand, might be different. It has to be chosen in appropriate fashion such that both solutions match properly at $\overline{Q}$.

For a sufficiently high barrier the particles inside the potential well may be assumed to stay close to a local equilibrium associated to the temperature T. In case that the corresponding fluctuations $\langle\Delta Q^2\rangle_a^{\rm eq}$ concentrate on a region around the minimum, the potential may be replaced by a harmonic oscillator and the associated local phase-space density may be approximated by

$$f_a(Q,P)\equiv f(Q\approx Q_a,P) =\mathcal{N}_a\exp\left[-\beta\left(\frac{P^2}{2M_a}+V(Q_a)+\frac{C_a}{2}(Q-Q_a)^2\right)\right]. \tag{A14}$$

This is a reasonable estimate up to a $\overline{Q}$ with

$$(\overline{Q}-Q_a)^2\gtrsim\langle\Delta Q^2\rangle_a^{\rm eq}\equiv\frac{T}{C_a}. \tag{A15}$$

Likewise, approximating the barrier by an inverted oscillator, the phase-space density may be represented by Kramers's stationary solution [7,10] (neglecting any quantum effects, see, e.g., [6])

$$f_b(Q,P)\equiv f(Q\approx Q_b,P)$$
$$=\mathcal{N}_b\exp\left[-\beta\left(\frac{P^2}{2M_b}+V(Q_b)-\frac{|C_b|}{2}(Q-Q_b)^2\right)\right]$$
$$\times\int_{-\infty}^{P-A(Q-Q_b)}du\frac{1}{\sqrt{2\pi\sigma}}\exp\left(-\frac{u^2}{2\sigma}\right), \qquad \text{(A16)}$$

where

$$A=\frac{|C_b|}{\varpi_b(\sqrt{1+\eta_b^2}-\eta_b)}$$

and

$$\sigma=TM_b\left(\frac{1}{(\sqrt{1+\eta_b^2}-\eta_b)^2}-1\right). \qquad \text{(A17)}$$

This latter solution must be joined to the one given by Eq. (A14) in some intermediate region, say at $\overline{Q}$. It would be too much to require this to be possible for *any P*, in particular, as we are not able to treat the inertia in continuous fashion, for reasons given above. However, as the rate is determined by the ratio of two quantities which are averaged over momentum it turns out sufficient to match only the reduced *Q*-space densities. As suggested by Eq. (A7), the latter are obtained by integrating out the momentum *P* in Eqs. (A14) and (A16) to get

$$n_a(Q)=\mathcal{N}_a\sqrt{2\pi M_aT}\exp\left[-\beta\left(V(Q_a)+\frac{C_a}{2}(Q-Q_a)^2\right)\right] \qquad \text{(A18)}$$

and

$$n_b(Q)=\mathcal{N}_b\sqrt{\frac{\pi M_bT}{2}}\exp\left[-\beta\left(V(Q_b)-\frac{|C_b|}{2}(Q-Q_b)^2\right)\right]$$
$$\times\left[1+\mathrm{erf}\left(\sqrt{\frac{|C_b|}{2T}}(Q-Q_b)\right)\right]. \qquad \text{(A19)}$$

To obtain the last expression identities for error functions have been applied. Still it is not of a form for which a condition, such as $n_a(\overline{Q})=n_b(\overline{Q})$ would make much sense. For this we need the additional assumption

$$|C_b|(\overline{Q}-Q_b)^2\gg T, \qquad \text{(A20)}$$

which renders the error function in Eq. (A19) close to unity. Then the two densities match smoothly at a $\overline{Q}$ satisfying

$$V(Q_a)+\frac{C_a}{2}(\overline{Q}-Q_a)^2=V(Q_b)-\frac{|C_b|}{2}(\overline{Q}-Q_b)^2, \qquad \text{(A21)}$$

if only the normalization constants are chosen according to

$$\mathcal{N}_a=\mathcal{N}_b\sqrt{\frac{M_b}{M_a}}. \qquad \text{(A22)}$$

Now we are in a position to calculate the rate from Eq. (A12). Plugging Eq. (A22) into Eq. (A14) the number of "particles" at the minimum (A13) becomes

$$N_a\approx\mathcal{N}_b\sqrt{2\pi M_bT}\sqrt{\frac{2\pi T}{C_a}}\exp[-\beta V(Q_a)]$$
$$=\mathcal{N}_b2\pi T\sqrt{\frac{M_b}{C_a}}\exp[-\beta V(Q_a)]. \qquad \text{(A23)}$$

To get this simple expression it was assumed that the Δ, which in Eq. (A13) defines the range of integration, is of the order of or larger than the fluctuation $\langle\Delta Q^2\rangle_a^{\mathrm{eq}}$ given in Eq. (A15), such that the Gaussian integral can be calculated for $\Delta\to\infty$. The current at the barrier may be evaluated from Eqs. (A16) and (A6) with $Q=Q_b$. After a lengthy but straightforward calculation involving identities for error integrals, once more, one arrives at

$$j_b=\mathcal{N}_bT\sqrt{\frac{M_b}{|C_b|}}\varpi_b(\sqrt{1+\eta_b^2}-\eta_b)\exp[-\beta V(Q_b)]. \qquad \text{(A24)}$$

From Eqs. (A24) and (A23) the decay rate (A12) turns into

$$R_K^{hv}=\frac{\varpi_b}{2\pi}\sqrt{\frac{C_a}{|C_b|}}(\sqrt{1+\eta_b^2}-\eta_b)\exp(-\beta E_b)$$
$$=\frac{\varpi_a}{2\pi}\sqrt{\frac{M_a}{M_b}}(\sqrt{1+\eta_b^2}-\eta_b)\exp(-\beta E_b), \qquad \text{(A25)}$$

confirming the expression (6) used in the text. We may note again that the result (A25) was derived earlier in [15] within an extension of the perturbed static path approximation (PSPA).

Finally, we like to come back once more to the conditions (A15) and (A20) imposed before. They go along with the relation (A21) for $\overline{Q}$ and the barrier height $E_b=V(Q_b)-V(Q_a)$. The latter must then satisfy $E_b=C_a/2(\overline{Q}-Q_a)^2+|C_b|/2(\overline{Q}-Q_b)^2\gg T$. It may be useful to visualize these relations with the help of the following schematic potential:

$$V(Q)=\begin{cases}V(Q_a)+\dfrac{C_a}{2}(Q-Q_a)^2 & \text{for } Q<\overline{Q},\\[2ex] E_b+V(Q_a)-\dfrac{|C_b|}{2}(Q-Q_b)^2 & \text{for } Q>\overline{Q}.\end{cases} \qquad \text{(A26)}$$

Choosing the $\overline{Q}$ according to $\overline{Q}=(C_aQ_a+|C_b|Q_b)/(C_a+|C_b|)$ the two parabolas match smoothly with a continuous first derivative. Possible errors related to Eqs. (A15) and (A20) may easily be estimated from elementary properties of the error function.

2. The relation to the transition state result

In transition state theory one assumes a system that is totally equilibrized inside the barrier and for which, at the barrier, current only flows outward discarding any backflow. Within its most general version, the fission rate has been estimated by Bohr and Wheeler through their famous formula [27]. There the equilibrium is the one of a microcanonical ensemble as represented by the density of states (of the total system at the minimum and of the intrinsic system at the barrier). To the extent that the microcanonical ensemble may be represented by a canonical one, with one and the same temperature at the minimum and at the barrier, the calculation of the rate can be done as follows, looking only at the collective degree of freedom. The outward current (at the barrier) is given by

$$j_b^{trans} = \int_0^\infty dP \frac{P}{M_b} f_{eq}(Q_b, P) \propto \int_{-\infty}^\infty dP \frac{P}{M_b} \exp\left(-\beta \frac{P^2}{2M_b} \right) \Theta(P). \quad \text{(A27)}$$

Comparing with Kramers's stationary solution shown in Eq. (A16) one realizes [34] the only difference the replacement of the theta function $\Theta(P)$ of Eq. (A27) by the integral (for $Q = Q_b$) which appears in the second line of Eq. (A16). Due to the following representation of the Θ function

$$\Theta(P) = \lim_{\sigma \to 0} \int_{-\infty}^P du \frac{1}{\sqrt{2\pi\sigma}} \exp\left(-\frac{u^2}{2\sigma} \right), \quad \text{(A28)}$$

it is seen that (for finite temperature)

$$R_{trans} = R_K^{hv}(\eta = 0). \quad \text{(A29)}$$

This follows immediately with the help of the expression given for σ in Eq. (A17).

3. The Smoluchowski limit

Performing in Eq. (A25) the limit $\eta_b \gg 1$, with the effective damping rate defined by (2), one gets

$$R_K^{hv} \to \frac{\varpi_b}{2\pi} \sqrt{\frac{C_a}{|C_b|}} \frac{1}{2\eta_b} \exp(-\beta E_b) = \frac{1}{2\pi} \frac{1}{\gamma_b} \sqrt{C_a |C_b|} \exp(-\beta E_b) = R_{\text{ovd}}. \quad \text{(A30)}$$

This expression coincides with the formula (10) associated above with the Smoluchowski limit. As a matter of fact, this result can be obtained directly from the Smoluchowski equation

$$\frac{\partial}{\partial t} n(Q,t) = \frac{\partial}{\partial Q} \left(\frac{1}{\gamma(Q)} \frac{\partial V(Q)}{\partial Q} + \frac{T}{\gamma(Q)} \frac{\partial}{\partial Q} \right) n(Q,t) = \frac{\partial}{\partial Q} j(Q,t). \quad \text{(A31)}$$

The calculation of the decay rate is quite easy in this case. Indeed, Eq. (A31) gives an explicit form of the $j(Q,t)$ as a function of the density $n(Q,t)$. Although in our case the friction coefficient varies with Q the common derivation of the rate formula (see, e.g., [35]) may be taken over without much difficulties.

Notice that the transition from an equation like Eqs. (A1)–(A31) only requires the $\eta(Q)$ to be large enough at *any* Q. Such a transition may be performed also in the case of a variable inertia, at least if condition (A11) is fulfilled. In any case, in the overdamped limit the inertia has to drop out. We may note in passing that this transition is in accord with the locally harmonic approximation in the form discussed in Sec. 2.2.5 of [6]. Following the arguments of Sec. 10.1 and 10.4 of [35], Eq. (A31) can strictly be derived from Eq. (A1) neglecting the term (A8).

4. Strutinsky's derivation of the rate formula

The essential idea exploited in Ref. [14] is written there below Eq. (6). Different than the approach described in Sec. A 1 , the number of particles N_a at the minimum is estimated by multiplying the density $n_b(Q)$ of Kramers's stationary solution calculated at Q_a by an "effective length," which in turn is determined by the mean fluctuation of the oscillator at this Q_a times $\sqrt{2\pi}$, viz. by

$$\sqrt{2\pi}(\Delta Q)_{\text{eq}} = \sqrt{\frac{2\pi T}{C_a}}. \quad \text{(A32)}$$

(The additional factor $\sqrt{2\pi}$ is required to ensure the appropriate measure needed for the normalization of a Gaussian.) In this way one gets from Eqs. (A24) and (A19)

$$R_K^{hv} = \frac{\varpi_b}{2\pi} \sqrt{\frac{C_a}{|C_b|}} (\sqrt{1+\eta_b^2} - \eta_b) \exp(-\beta E_b). \quad \text{(A33)}$$

Here, it was assumed (i) that the $Q_b - Q_a$ is sufficiently large such that in (A19) the error function could be replaced by unity, and (ii) that the barrier height can be estimated as $E_b \approx (|C_b|/2)(Q_a - Q_b)^2$. The result (A33) has the same form as given in Eq. (A25). As explained earlier, it is equivalent to Eq. (6) or the second line of Eq. (A25) that involve the inertias. This latter expression is identical to the one given in Eq. (16) of [14] if *one only interchanges there primed and unprimed quantities*.

APPENDIX B: A SCHEMATIC MICROSCOPIC MODEL

1. The Lorentz model for intrinsic motion

Let us assume that the nucleonic excitations can be parametrized by the response function (in this section we set $\hbar = 1$)

$$\chi(\omega) = -\overline{F^2} \left[\frac{1}{\omega - \Omega + i\Gamma/2} - \frac{1}{\omega + \Omega + i\Gamma/2} \right]. \quad \text{(B1)}$$

Here, the average matrix element $\overline{F^2}$ of the one body operator $\hat{F}$, which acts as the generator of collective motion, mea-

sures the overall strength of the distribution. The states reached by that coupling are centered at Ω with an effective bandwidth Γ (measured here in units of MeV/$\hbar$). For real frequencies the reactive and dissipative response functions, χ' and χ'', are readily calculated noticing that they represent real and imaginary parts of $\chi(\omega)=\chi'(\omega)+i\chi''(\omega)$. The static response is given by

$$\chi(0)=\frac{2\Omega\overline{F^2}}{\Omega^2+(\Gamma/2)^2}=\chi'(\omega=0). \tag{B2}$$

It is useful to rewrite this (intrinsic) response function $\chi(\omega)$ in terms of the form of the oscillator response given in Eq. (12),

$$\chi(\omega)=\frac{-2\Omega\overline{F^2}}{\omega^2+i\Gamma\omega-[\Omega^2+(\Gamma/2)^2]}=\frac{-1/M_{\rm int}}{\omega^2+i\Gamma_{\rm int}\omega-\varpi_{\rm int}^2}. \tag{B3}$$

In this way transport coefficients for intrinsic motion appear

$$M_{\rm int}=\frac{1}{2\Omega\overline{F^2}},\quad \Gamma_{\rm int}=\Gamma,\quad \varpi_{\rm int}^2=\Omega^2+(\Gamma/2)^2. \tag{B4}$$

Next we turn to the collective response. For the F mode it is given by [6]

$$\chi_{\rm coll}(\omega)=\frac{\chi(\omega)}{1+k\chi(\omega)}=\frac{1}{\frac{1}{\chi(\omega)}+k}=\frac{-1/M_F}{\omega^2+i\Gamma_F\omega-\varpi_F^2}, \tag{B5}$$

with the inverse coupling constant

$$-\frac{1}{k}=C(0)+\chi(\omega=0) \tag{B6}$$

and $C(0)$ being the stiffness of the free energy. The transport coefficients for the collective F mode are

$$M_F=M_{\rm int},\quad \Gamma_F=\Gamma_{\rm int},\quad C_F\equiv M_F\varpi_F^2=M_{\rm int}\varpi_{\rm int}^2+k. \tag{B7}$$

To get the transport coeffecients for the Q-mode one needs to multiply these quantities by $1/k^2$. For slow modes it so turns out that to a good approximation the $C(0)$ in Eq. (B6) may be neglected as compared to the $\chi(0)$. This leads to

$$M=\frac{1}{k^2}M_F\approx\frac{[\chi(0)]^2}{2\Omega\overline{F^2}}=\frac{2\Omega\overline{F^2}}{[\Omega^2+(\Gamma/2)^2]^2}=\frac{\chi(0)}{\Omega^2+(\Gamma/2)^2}=\frac{1}{2}\frac{\partial^2\chi'}{\partial\omega^2}\bigg|_{\omega=0}. \tag{B8}$$

In the last expression we have made use of Eq. (B2). Last but not least this has been done because the static response seems to be quite insensitive to the increase of the temperature [36], at least for not too large T. The transformation from the F to the Q mode leaves ratios between transport coefficients unchanged. The collective width and the ratio between friction and inertia, thus becomes $\Gamma_{\rm kin}=\Gamma$. For friction this implies

$$\gamma=\Gamma_{\rm kin}M=\frac{\Gamma}{\Omega^2+(\Gamma/2)^2}\chi(0)=\frac{\partial\chi''}{\partial\omega}\bigg|_{\omega=0} \tag{B9}$$

and for the stiffness one gets the expected result $C\approx C(0)$, which follows because the C_F of Eq. (B7) can be written as

$$C_F=M_F\varpi_F^2=\frac{1}{\chi(0)}+k=\frac{C(0)}{\chi(0)[C(0)+\chi(0)]}\approx\frac{C(0)}{[\chi(0)]^2}. \tag{B10}$$

The second equation follows from Eqs. (B4) and (B2).

Finally, we should like to note that for the schematic model with only one mode the inertia always is the one which defines the value of the energy weighted sum. Likewise, as one may see from Eq. (B9) for friction and (to lesser extent) from Eq. (B8) for the inertia, these transport coefficients are well represented by their ''zero frequency limits.''

2. Benefits and shortcomings of this model

a. Weak damping

For this model weak damping is defined as $\Omega\gg\Gamma/2$. In this case static response and inertia turn into the expressions known from the so called ''degenerate model'' [21] $\chi(0)=2\overline{F^2}/\Omega$ and $M=2\overline{F^2}/\Omega^3$. Notice where in the inertia has the typical structure of the cranking inertia. For friction one gets $\gamma=2\Gamma\overline{F^2}/\Omega^3$.

The degenerate model becomes most transparent if it is applied to the case wherein nucleons move in oscillator potentials, in particular, if any spin dependent forces are neglected. Then the intrinsic excitation is given by $\hbar\Omega=\Delta N\hbar\Omega_0\equiv\Delta N(41\ \text{MeV}/A^{1/3})$, where ΔN is the difference in the major quantum numbers of those states that are coupled through the multipole operator F. Whereas for the quadrupole there is only one possibility, namely $\Delta N=2$, this is no longer true for other multipoles, for which more than just one mode are possible. The same holds true as soon as a spin orbit force is introduced. Then even for the quadrupole transitions with $\Delta N=0$ are possible. It is them that lead to the low frequency modes we are typically interested in, as they resemble closest the fission mode. If one still likes to stick to the (degenerate or) Lorentz model—which only allows for one mode—the effective frequency Ω will only be a fraction of the shell spacing parameter Ω_0.

b. Strong damping

It is tempting to apply this schematic model also to the extreme case of very strong damping when Γ becomes comparable to or larger than the frequency Ω of the typical intrinsic excitation. Plain confidence in the formula (B9) would lead to $\gamma\simeq(4/\Gamma)\chi(0)$. This seems particularly intriguing if

on the one hand the static response does indeed not change much with T, and if, on the other hand, the Γ is associated to the widths of the single particle states, as will be discussed below. According to Eq. (B13) there might then be some range in which the friction force would show the typical $1/T^2$ dependence one expects for liquids in the "collision dominated regime," see also Sec. 5.3 of Ref. [17]. However, we claim that for finite nuclei the situation is more complicated. Evidently, the effects of strong collisions are due to the increasing importance of residual interactions. But the latter imply other consequences as well, last but not least a mixing with more complicated states such that with increasing thermal excitations many-particle–many-hole states become more and more important. As has been demonstrated in previous papers, see, e.g., [13,6] amongst others, this effect implies that high frequency modes shift to lower frequencies such that the typical mode at stake in the transport model gets more and more strength—implying that finally its inertia is given by the sum rule limit. Moreover, it has been demonstrated that this feature goes along with the disappearance of shell effects at $T=T_{\rm shell}$. This problem is addressed in the text.

c. Temperature dependence through collisional damping

Looking back at the intrinsic response function introduced in Eq. (B1), one realizes that the only quantity that can be expected to change sensitively with excitation is the width Γ. To get some first orientation we may relate it to the single particle width. For a Fermi system the latter can be expected to be of the form[2] [6]

$$\Gamma_{\rm sp}(\omega,T)=\frac{1}{\Gamma_0}\,\frac{(\omega-\mu)^2+\pi^2T^2}{1+[(\omega-\mu)^2+\pi^2T^2]/c^2}, \qquad \text{(B11)}$$

with the parameters

$$\frac{1}{\Gamma_0}=0.03\ \ \text{MeV}^{-1}\ \ \text{and}\ \ \ c=20\ \ \text{MeV}. \qquad \text{(B12)}$$

For slow collective motion we may omit the frequency dependence and evaluate this width at the Fermi surface and put $\omega-\mu=0$ in Eq. (B11). Along this approximation we may put

$$\Gamma_{\rm kin}\approx 2\Gamma_{\rm sp}(\mu,T)\approx\frac{0.6T^2}{1+T^2/40}\quad (T\ \text{in MeV}). \qquad \text{(B13)}$$

Evidently the correction term in the denominator only becomes important at temperatures of the order of $T\simeq 6$ MeV. This is already beyond that value were the other effects come into play we discussed in Sec. B 2 b. For this reason the actual $\Gamma(T)$ is changed in the main text.

Finally we may note that our schematic model is not capable of accounting for pairing. The latter will modify the transport properties at temperatures below $T\simeq T_{\rm pair}$. This is discussed in the text.

[2]Different than the notation used in [6], here energies are measured with respect to the Fermi surface μ.

[1] D. J. Hofman, B. B. Back, I. Diószegi, C. P. Montoya, S. Schadmand, R. Varma, and P. Paul, Phys. Rev. Lett. **72**, 470 (1994); see also P. Paul and M. Thoennessen, Annu. Rev. Nucl. Part. Sci. **44**, 65 (1994).

[2] D. J. Hofman, B. B. Back, and P. Paul, Phys. Rev. C **51**, 2597 (1995).

[3] B. B. Back *et al.*, Phys. Rev. C **60**, 044602 (1999).

[4] I. Diószegi, N. P. Shaw, I. Mazumdar, A. Hatzikoutelis, and P. Paul, Phys. Rev. C **61**, 024613 (2000).

[5] G. Rudolf and A. Kelić, Nucl. Phys. **A679**, 2516 (2001).

[6] H. Hofmann, Phys. Rep. **284**, 137 (1997).

[7] H. A. Kramers, Physica (Amsterdam) **7**, 284 (1940).

[8] H. Hofmann and F. A. Ivanyuk, Phys. Rev. Lett. **82**, 4603 (1999).

[9] F. A. Ivanyuk and H. Hofmann, Nucl. Phys. **A657**, 19 (1999).

[10] P. Hänggi, P. Talkner, and M. Borkovec, Rev. Mod. Phys. **62**, 251 (1990).

[11] A. Bulgac, G. Do Dang, and D. Kusnezov, Physica E (Amsterdam) **9**, 429 (2001); E. Lutz and H. A. Weidenmüller, Physica A **267**, 354 (1999).

[12] M. Brack, J. Damgaard, A. S. Jensen, H. C. Pauli, V. M. Strutinsky, and C. Y. Wong, Rev. Mod. Phys. **44**, 320 (1972); see also T. Ledergerber and H. C. Pauli, Nucl. Phys. **A207**, 1 (1973).

[13] H. Hofmann, S. Yamaji, and A. S. Jensen, Phys. Lett. B **286**, 1 (1992).

[14] V. M. Strutinsky, Phys. Lett. **47B**, 121 (1973).

[15] C. Rummel (unpublished); C. Rummel and H. Hofmann Phys. Rev. E (to be published).

[16] S. Yamaji, H. Hofmann, and R. Samhammer, Nucl. Phys. **A475**, 487 (1988).

[17] H. Hofmann, F. A. Ivanyuk, and S. Yamaji, Nucl. Phys. **A598**, 187 (1996).

[18] S. Yamaji, F. A. Ivanyuk, and H. Hofmann, Nucl. Phys. **A612**, 1 (1997).

[19] F. A. Ivanyuk, H. Hofmann, V. V. Pashkevich, and S. Yamaji, Phys. Rev. C **55**, 1730 (1997); nucl-th/9701032.

[20] F. A. Ivanyuk, Acta Phys. Slov. **49**, 53 (1999).

[21] A. Bohr and B.R. Mottelson, *Nuclear Structure* (Benjamin, London, 1975), Vol. II.

[22] C. Guet, E. Strumberger, and M. Brack, Phys. Lett. B **205**, 427 (1988).

[23] A. G. Magner, S. Vydrug-Vlasenko, and H. Hofmann, Nucl. Phys. **A524**, 31 (1991).

[24] M Hunyadi *et al.* (unpublished)

[25] S. Bjornholm and L. E. Lynn, Rev. Mod. Phys. **52**, 725 (1980).

[26] M. Thoennessen and G. F. Bertsch, Phys. Rev. Lett. **71**, 4303 (1993).

[27] N. Bohr and J. A. Wheeler, Phys. Rev. **56**, 426 (1939).

[28] P. J. Siemens and A.S. Jensen, *Elements of Nuclei: Many-Body Physics with the Strong Interaction* (Addison-Wesley, New York, 1987).
[29] R. Vandenbosch and J.R. Huizenga, *Nuclear Fission* (Academic, London, 1973).
[30] M. Thoennessen, Nucl. Phys. **A599**, 1 (1996).
[31] H. A. Weidenmüller and J.-S. SDZhang, Phys. Rev. C **29**, 879 (1984).
[32] A. S. Jensen, H. Hofmann, and P. Siemens, in *Nucleon-Nucleon Interaction and the Nuclear Many-Body Problems*, edited by S. S. Wu and T. T. S. Kuo (World Scientific, Singapore, 1984).
[33] H. Hofmann and C. Ngô, Phys. Lett. **65B**, 97 (1976); C. Ngô and H. Hofmann, Z. Phys. A **282**, 83 (1977).
[34] One of us (H.H.) gratefully acknowledges an enlightening discussion with W.J. Swiatecki on this subject.
[35] H. Risken, *The Fokker-Planck–Equation* (Springer-Verlag, Berlin/Heidelberg, 1989).
[36] D. Kiderlen, H. Hofmann, and F. A. Ivanyuk, Nucl. Phys. **A550**, 473 (1992).